RHEUMATOLOGY

Rheumatology 2011;50:1033–1044
doi:10.1093/rheumatology/keq423
Advance Access publication 21 January 2011

Original article

Distinct *in vitro* binding properties of the anti-CD20 small modular immunopharmaceutical 2LM20-4 result in profound and sustained *in vivo* potency in cynomolgus monkeys

Cheryl Nickerson-Nutter[1], Lioudmila Tchistiakova[2], Nilufer P. Seth[1], Marion Kasaian[1], Barbara Sibley[1,†], Stephane Olland[2], Richard Zollner[2], William A. Brady[3], Kendall M. Mohler[3], Peter Baum[3], Alan Wahl[3], Deborah Herber[1], Yulia Vugmeyster[4], David Wensel[4], Neil M. Wolfman[1], Davinder Gill[2], Mary Collins[1] and Kyri Dunussi-Joannopoulos[1]

Abstract

Objectives. To characterize the *in vitro* binding and effector function properties of CD20-directed small modular immunopharmaceutical (SMIP) 2LM20-4, and to compare its *in vivo* B-cell depletion activity with the mutated 2LM20-4 P331S [no *in vitro* complement-dependent cytotoxicity (CDC)] and rituximab in cynomolgus monkeys.

Methods. Direct binding is examined in flow cytometry, confocal microscopy, scatchard and lipid raft assays. Effector function assays include CDC and Fc-mediated cellular toxicity. In the 6-month-long *in vivo* B-cell depletion study, single i.v. dosages of 1 or 10 mg/kg of anti-CD20 proteins were administered to monkeys and B-cell counts were monitored in peripheral blood, bone marrow and lymph nodes.

Results. 2LM20-4 has lower saturation binding to human primary B cells and recruits fewer CD20 molecules into lipid rafts compared with rituximab; however, it induces higher *in vitro* CDC. In competitive binding, 2LM20-4 only partially displaces rituximab, suggesting that it binds to a fraction of CD20 molecules within certain locations of the plasma membrane as compared with rituximab. In monkeys, 2LM20-4 had more sustained B-cell depletion activity than rituximab in peripheral blood and had significantly more profound and sustained activity than 2LM20-4 P331S and rituximab in the lymph nodes.

Conclusions. SMIP 2LM20-4, which binds to a fraction of CD20 molecules as compared with rituximab, has more potent *in vitro* CDC, and more potent and sustained B-cell depletion activity in cynomolgus monkeys. Our work has considerable clinical relevance since it provides novel insights related to the emerging B-cell depletion therapies in autoimmune diseases.

Key words: B-cell depletion, Autoimmune diseases, Anti-CD20 small modular immunopharmaceutical, *In vitro* properties, *In vivo* properties.

BASIC SCIENCE

[1]Inflammation and Immunology, [2]Global Biological Technologies, Pfizer Biotherapeutics Research and Development, Cambridge, MA, [3]Trubion Pharmaceuticals Inc., Seattle, WA and [4]Global Drug Safety and Metabolism, Pfizer Biotherapeutics Research and Development, Andover, MA, USA.

Submitted 29 June 2010; revised version accepted 23 November 2010.

Correspondence to: Kyri Dunussi-Joannopoulos, Inflammation and Immunology, Pfizer Biotherapeutics Research and Development, 200 Cambridge Park Drive, Cambridge, MA 02140, USA.
E-mail: kyri.dunussi-joannopou@pfizer.com

[†]Deceased.

Introduction

During the past decade, B cells have convincingly emerged as critical players in the pathogenesis of autoimmune disorders and novel therapeutic modalities targeting B cells have been proven to be effective in autoimmune diseases like RA and SLE [1–5]. To date, selective B-cell depletion with the use of mAbs has shown much promise in RA, and rituximab, a chimeric mAb that binds to CD20 on B cells, is an Food and Drug

Administration-approved treatment for RA patients who failed to respond to anti-TNF therapies [6]. B-cell depletion has also shown promising efficacy in SLE, multiple sclerosis (MS) and autoimmune type I diabetes [7–13]; however, confirmation of this efficacy in controlled trials has not yet been reported.

Anti-CD20 mAbs have been previously characterized as either type I (rituximab-like), based on their ability to recruit CD20 molecules into detergent-insoluble microdomains and to activate complement-dependent cytotoxicity (CDC), or type II (tositumomab/B1-like), based on their ability to promote programmed cell death (PCD), but not CDC [14, 15]. Potent CDC was thought to be primarily related to the slow off-rate of the anti-CD20 mAb; however, it has been recently demonstrated that the CD20 epitope recognized by the mAb is also another critical factor for the induction of potent CDC [16]. Numerous *in vitro* studies have demonstrated that rituximab bound to $CD20^+$ B lymphoma cells redistributes CD20 molecules into lipid rafts and mediates CDC, Fc-mediated cellular toxicity and PCD in certain cell lines [17]. Also, pre-clinical *in vivo* studies indicate that both CDC and Fc-mediated cellular toxicity can contribute to mAb-induced tumour cell lysis [18–22]. However, evidence related to the relative clinical importance of each mechanism, and whether they are synergistic or antagonistic, is still conflicting [15]. The mechanism by which rituximab causes B-cell depletion in patients with RA and SLE is even more controversial [15, 23], and, to date, it is still not known to what extent CDC contributes to the success of anti-CD20 therapies in RA [24]. The need to elucidate the mechanistic pathways governing the success of B-cell depletion in the clinic instigated the engineering of B-cell-depleting reagents with modified effector function properties, and several such drug candidates are currently being evaluated in the clinic [5, 15, 25].

2LM20-4 is a humanized anti-CD20 small modular immunopharmaceutical (SMIP) protein drug candidate that is smaller than an antibody and is being developed for the treatment of patients with autoimmune disorders. *In vitro* binding and competition assays indicate that 2LM20-4 binds only to a fraction of CD20 molecules within certain locations of the plasma membrane in human primary B cells; however, it mediates more potent CDC activity compared with rituximab. 2LM20-4 does not induce *in vitro* PCD, but in the presence of effector cells, it potentiates Fc-mediated cellular toxicity comparable with rituximab. Notably, due to the decreased *in vitro* direct binding of 2LM20-4, its inability to saturate CD20 on the surface of primary B-cells, off-rate, competition and lipid raft distribution assays, we would predict a lower *in vivo* potency compared with rituximab. To elucidate how these *in vitro* binding properties correlate with *in vivo* efficacy, we compared 2LM20-4 with rituximab in a non-human primate study. Also, considering the controversial role of complement activation in B-cell depletion in autoimmune diseases, we generated a variant 2LM20-4 with mutation P331S in the Fc domain (2LM20-4 P331S), known to reduce C1q binding and complement activation, and used it as a comparator in the same study. We present here that 2LM20-4 has significantly more potent and sustained activity in the peripheral blood and the lymph nodes compared with rituximab. Also, we show here that mutation P331S significantly reduces B-cell depletion activity in lymphoid tissues of cynomolgus monkeys. Overall, our results suggest that 2LM20-4 has a unique combination of *in vitro* binding and effector function properties that cannot be characterized as either type I or type II and can lead to profound *in vivo* B-cell depletion activity in cynomolgus monkeys.

Materials and methods

Generation of 2LM20-4 and 2LM20-4 P331S SMIP constructs

2LM20-4 was generated based on the mouse mAb 2H7, which recognizes an extracellular loop of the human CD20 B-cell surface molecule [26, 27]. The variable regions of 2H7 were humanized by complementarity-determining region (CDR) grafting and converted into a single-chain variable fragment (scFv) variable light–variable heavy chain (VL–VH) format using a flexible (Gly_4–Ser) 16-amino-acid linker. 2LM20-4 SMIP protein was constructed by fusing coding regions of humanized scFv with human Immunoglobulin G1 heavy chain constant region 2 (CH2) and heavy chain constant region 3 (CH3) domains through the modified human IgG1 hinge sequence: EPKSSDKTHTCPPCP. To generate 2LM20-4 P331S, proline at position 331 was changed to serine in the constant fragment (Fc) region by PCR mutagenesis. Coding regions were sub-cloned into pSMED2 mammalian expression vector and expressed in stable Chinese hamster ovary (CHO) cell lines. Proteins were purified using a Protein A–Sepharose FF column. A size exclusion chromatography (SEC) column was used to remove aggregates. The purity and molecular weight of proteins were confirmed by SDS–PAGE, analytical SEC and light-scatter analysis.

In vitro binding to primary B cells

Normal human primary B cells were isolated from buffy coats by negative selection (RosetteSep human B cell enrichment kit; StemCell Technologies, Vancouver, BC, Canada) and were incubated with varying concentrations of anti-CD20 proteins or a control IgG1 antibody for 30 min on ice. A phycoerythrin-labelled anti-IgG antibody (SouthernBiotech, Birmingham, AL, USA) was used for detection of the anti-CD20 molecules, and 7-amino-actinomycin D (7AAD; BD Biosciences, San Jose, CA, USA) for exclusion of dead cells. Cells were analysed on LSR II (Becton Dickinsosn, San Jose, CA, USA) and data analysis was performed using FlowJo software 7.2.2 (TreeStar Inc., Ashland, OR, USA).

Confocal microscopy

Primary human B cells were pre-treated for 10 min at room temperature (RT) with 250 nM control human IgG1 and then treated for 10 min at RT with biotinylated 2LM20-4, rituximab or isotype control antibody. Cells were washed

and stained with Alexa Fluor 568-streptavidin (Invitrogen, Carlsbad, CA, USA) for 30 min at 4°C. Cells were washed, spun onto microscope cover slips, fixed with Cytofix-cytoperm (BD Biosciences, San Jose, CA, USA), washed in 1 : 2 perm/wash (BD Biosciences), and then stained with TO-PRO 3 (Invitrogen). Cover slips were mounted using Pro-Long (Invitrogen), and set overnight at RT. Slides were read using a Nikon TE-300 microscope (Nikon Instruments Inc., Melville, NY, USA) with Bio-Rad Radiance 2000 confocal system.

Scatchard studies

Equilibrium dissociation constants (K_ds) were determined by radiolabelling 2LM20-4 and rituximab with ^{125}Iodine (1 nmol/0.5 mCi) using Pierce Iodotube tyrosine method (Thermo Fisher Scientific, Rockford, IL, USA) and plating them at 12 concentrations in triplicate (20 pM to 40 nM) ± 100 × unlabelled 2LM20-4 or rituximab in V-bottom 96-well tissue culture plates. Primary B cells were added to the plates (37 000–200 000 cells/well, depending on the donor) and the plates were incubated overnight. Cells were spun down, and cell pellets were solubilized with 100 μl 1 N NaOH for 10 min and were counted in a gamma counter (bound). GraphPad Prism software (GraphPad Software, La Jolla, CA, USA) was used for curve fitting. For competitive binding, a constant 5 nM ^{125}I-rituximab was combined with 12 concentrations of unlabelled 2LM20-4 ranging from 100 pM to 100 nM in triplicate.

Lipid rafts

To study the redistribution of CD20 molecules into low density, detergent-insoluble membrane microdomains (lipid rafts), we used the protocol previously described for rituximab [28]. Primary B cells or Ramos B lymphoma cells were incubated with iodinated 2LM20-4, rituximab or isotype control (1 μg/2 × 10^6 cells) at 37°C for 0–60 min. Cells were spun down, and cell pellets were lysed with ice-cold 0.5% Triton X-100 for 15 min. Lysates were spun down at 14 000 *g* for 15 min at 4°C to separate insoluble material. Soluble and insoluble lysate fractions were counted on a gamma counter followed by the determination of the distribution of radio labelled proteins in the soluble (monomeric or weakly associated with lipid rafts) *vs* insoluble (strongly associated with lipid rafts) fractions.

In vitro CDC assays

Primary human B cells were plated at 1 × 10^5 cells/well in media containing RPMI 1640, 4-(2-hydroxyethyl)-1-piperazineethanesulfonic acid and 10% normal human serum complement (Quidel, Santa Clara, CA, USA). Varying concentrations of SMIP proteins, rituximab or control antibody were added to the wells. After incubation for 3.5 h at 37°C in a 5% CO_2 incubator, the cells were stained with propidium iodide (PI). Data were acquired using the Becton Dickinson LSR II and analysed with FlowJo software 7.2.2.

In vitro Fc-dependent cellular cytotoxicity

Primary B cells (targets) and NK cells (effectors) were isolated from the same donor. B cells were labelled with 0.3 μM carboxy-fluorescein diacetate, succinimidyl ester (CFSE) for 15 min at 37°C and incubated with varying concentrations of the SMIP proteins or rituximab for 30 min at 37°C. NK cells were added at a 1 : 4 target: effector ratio to the wells. The cells were incubated for 4 h at 37°C and then stained with 7-AAD. Data were acquired using Becton Dickinson LSR II and analysed with FlowJo software 7.2.2.

Direct killing assay

Primary human B cells were treated with varying concentrations (0.01–500 nM) of 2LM20-4, 2LM20-4 P331S, rituximab or control antibody for 22 and 72 h at 37°C in a 5% CO_2 incubator. The cells were washed and stained with annexin V-allophycocyanin (APC) and PI, then washed again and analysed by flow cytometry on the BD LSR II. The percentage of live cells was calculated as cells that were negative for both annexin V and PI.

In vivo pharmacodynamic and pharmacokinetic study

Forty female naïve cynomolgus monkeys (*Macaca fascicularis*) were assigned to the study. The study was performed at a contract laboratory in accordance with the institution's Institutional Animal Care and Use Committee (IACUC) guidelines and was approved by Pfizer's Institutional Animal Care and Use Committee. The animals were acclimated for 14 days (A1–14). Groups (four monkeys/group) were administered single i.v. dosages of 1 or 10 mg/kg of anti-CD20 proteins according to Table 1.

Flow cytometric immunophenotyping was conducted on peripheral blood, lymph nodes and bone marrow samples using antibodies to CD3, CD19, CD20 and CD45 (CD3-FITC, CD19-APC, CD45-PE and CD20-APC; BD Pharmingen, San Diego, CA, USA).

Table 1 *In vivo* experimental protocol

Group	Test article	Dose (mg/kg)	Surgery	Number of animals
1	Vehicle	0	No	4
2	Rituximab	1	No	4
3[a]	Rituximab	10	Yes	4
4[b]	Rituximab	10	No	4
5	2LM20-4	1	No	4
6[a]	2LM20-4	10	Yes	4
7[b]	2LM20-4	10	No	4
8	2LM20-4 P331S	1	No	4
9[a]	2LM20-4 P331S	10	Yes	4
10[b]	2LM20-4 P331S	10	No	4

[a]Animals in Groups 3, 6 and 9 underwent surgery (bone marrow aspirates and lymph node biopsies). [b]Animals in Groups 4, 7 and 10 did not have bone marrow aspirates and lymph node biopsies and were included for the evaluation of the impact of surgery on peripheral blood results.

Statistical analysis

Log transformation was applied to the data on relative percent of $CD19^+$ lymphocytes before a linear mixed model analysis was performed. In the linear mixed model, the fixed effects included treatment group, day and their interaction. The correlation between repeated measurements on the same animals was modelled with a first-order autoregressive matrix. Contrasts in the framework of the linear mixed model were used for all comparisons.

Results

2LM20-4 and 2LM20-4 P331S have comparable binding to primary B cells

2LM20-4 was constructed based on the mAb 2H7. The modular design of SMIP molecules allows the combination of various antigen-binding domains with Fc domains of human antibodies through a flexible hinge sequence (Fig. 1A and B). 2LM20-4 and 2LM20-4 P331S had identical binding in all our flow cytometry binding assays (Fig. 1C). At the concentrations tested, rituximab reproducibly demonstrated higher saturation binding to human primary B cells compared with 2LM20-4 and 2LM20-4 P331S, as indicated by a higher mean fluorescence intensity (MFI). Confocal microscopy was also used to visualize the binding of biotinylated reagents to CD20 on primary B cells. Both rituximab and 2LM20-4 showed a diffuse staining pattern of binding over the cell surface, but cells stained with rituximab were significantly brighter compared with cells stained with 2LM20-4 or control antibody (Fig. 1D). These results suggest that 2LM20-4 may recognize only a proportion of CD20 molecules as compared with rituximab.

2LM20-4 has lower K_d and recruits fewer CD20 molecules than rituximab into lipid rafts

In direct binding studies with primary B cells using ^{125}I-labelled reagents, 2LM20-4 showed a K_d of 0.95 nM (Fig. 2A) and rituximab a K_d of 0.15 nM (Fig. 2B). Also, Scatchard plots for rituximab were linear and predicted 27 000 receptors/cell, whereas Scatchard plots for 2LM20-4 were curved and fitted non-linear regression for two-site binding (Fig. 2C). The lower level of binding by 2LM20-4 suggests that while it binds two sites, it does not bind either one to saturation. To test the degree of association of ^{125}I-2LM20-4 and ^{125}I-rituximab with CD20 molecules in lipid rafts, we followed the Triton X-100 solubilization protocol, previously used for the characterization of detergent-insoluble microdomains upon binding of rituximab to CD20 on B cells. The experiments were repeated several times using Ramos B cells and they reproducibly showed significantly higher per cent of Triton X-100 insoluble fraction for rituximab compared with 2LM20-4 (Fig. 2D). These results indicate that there are significant differences between the binding properties of 2LM20-4 and rituximab to CD20.

2LM20-4 shows partial displacement of rituximab in direct binding assays

In competitive direct binding assays, different amounts of cold competitor, up to a 20-fold excess, resulted in partial displacement of ^{125}I-rituximab on primary B cells (Fig. 3A). In flow cytometry direct binding assays, primary B cells were incubated for 1 h and overnight (Fig. 3B) with labelled anti-CD20 molecules and a 100-fold excess of unlabelled anti-CD20 molecules. Labelled 2LM20-4 was completely competed by excess unlabelled rituximab; however, labelled rituximab was only partially competed by excess unlabelled 2LM20-4, with a loss of diffuse cell surface staining by rituximab but maintenance of staining at cell: cell contacts. As expected, both excess cold rituximab and 2LM20-4 completely competed labelled rituximab and 2LM20-4, respectively. Similar findings were observed with confocal microscopy (Fig. 3C). A fluorescent signal was retained when staining with labelled rituximab and excess unlabelled 2LM20-4, whereas staining by labelled 2LM20-4 was completely abolished when excess unlabelled rituximab was present. These competition experiments suggest that, while rituximab and 2LM20-4 share an epitope on CD20, 2LM20-4 is able to compete with rituximab binding to CD20 only when rituximab is bound to CD20 in soluble areas of the plasma membrane.

Mutation P331S in the CH2 domain eliminates the *in vitro* CDC activity of 2LM20-4

The P331 residue has been previously identified as required for C1q binding to the Fc region of an IgG1 molecule [29]. In CDC assays performed using B cells from multiple healthy donors, 2LM20-4 demonstrated the highest CDC activity with a maximum of 80% of cell lysis, whereas 2LM20-4 P331S had no CDC activity and was similar to control antibody (Fig. 4A). Interestingly, rituximab showed 50% cell lysis and, therefore, lower CDC activity compared with 2LM20-4, despite the higher affinity and slower off rate of binding to CD20 on primary B cells (Fig. 4A).

2LM20-4 and 2LM20-4 P331S have comparable Fc-mediated cellular toxicity

2LM20-4, 2LM20-4 P331S and rituximab each demonstrated Fc-mediated cellular toxicity in a dose-dependent manner, as shown in Fig. 4B. Overall, 2LM20-4 had a trend of higher Fc-mediated cytotoxicity compared with rituximab, particularly at high concentrations; however, this finding never achieved statistical significance. These results indicate that 2LM20-4 induces potent Fc-mediated cytotoxicity and that the P331S mutation does not affect functional interactions of 2LM20-4 to FcγR receptors on human NK cells.

2LM20-4 and 2LM20-4 P331S do not induce direct killing of normal human B cells

It has been demonstrated that rituximab arrests cell growth and also causes apoptosis in some $CD20^+$ B-cell lines if cross-linked with a secondary anti-immunoglobulin antibody [30]. In a recent report, the type II anti-CD20

Fig. 1 2LM20-4 has a modular design and has lower saturation binding compared with rituximab. (**A**) Illustration of the structural domains of an antibody; dotted squares indicate the domains used for generation of the SMIP. (**B**) Structure of 2LM20-4. (**C**) Binding of 2LM20-4, 2LM20-4 P331S and rituximab to CD20 on primary human B cells. Similar results were obtained using several different donors; data from one donor are shown. (**D**) Confocal images showing binding of biotinylated 2LM290-4 or rituximab to primary B cells. Blue stain (TO-PRO 3) shows nuclear binding, red stain shows binding to CD20.

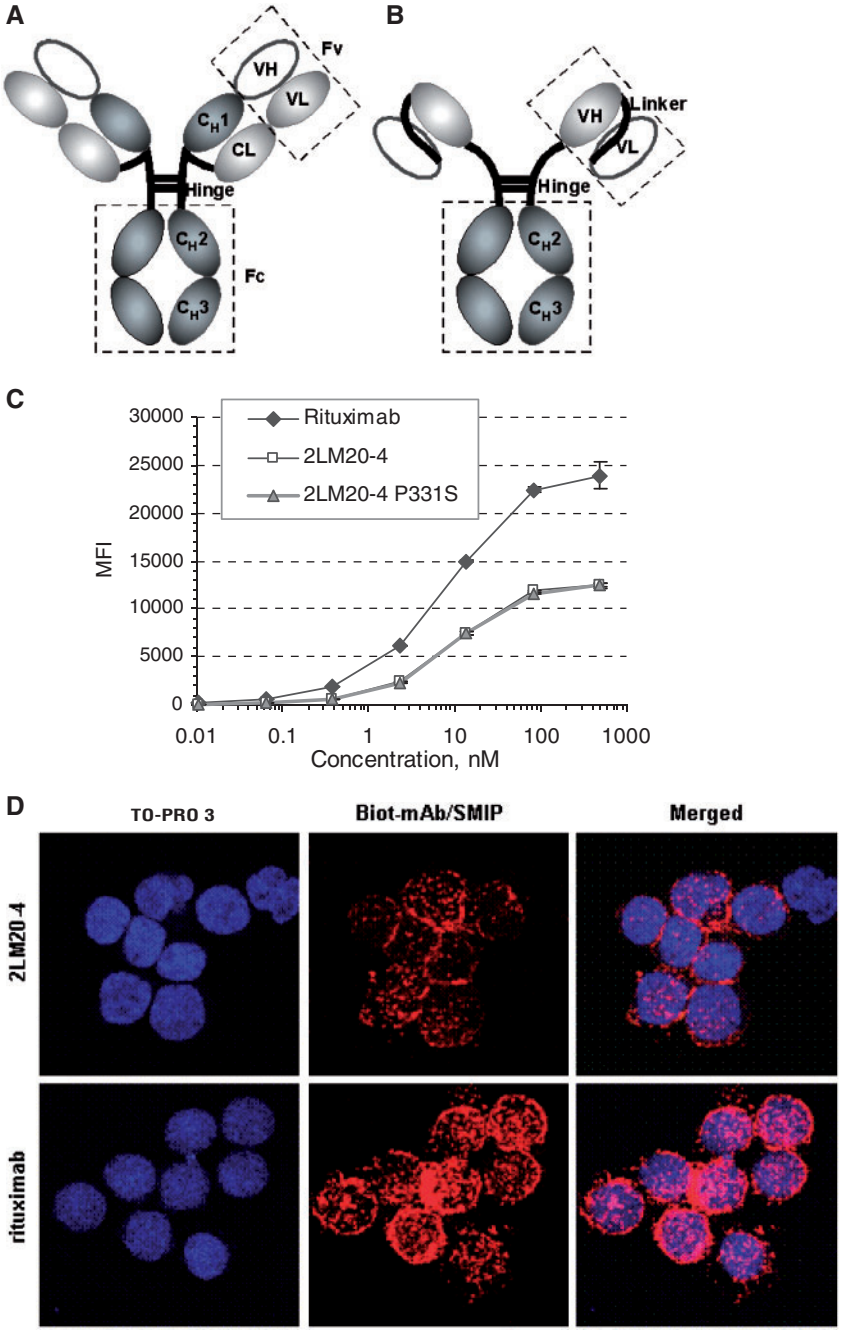

mAb tositumomab was able to induce a non-apoptotic mode of cell death in human B-cell lymphoma lines without secondary cross-linking [31]. Here, we performed PCD assays without secondary cross-linking. As shown in Fig. 4C, no specific killing of primary human B cells was observed at 22 h with varying concentrations of 2LM20-4, 2LM20-4 P331S or rituximab. Similarly, no specific killing of primary human B cells was observed at 72 h with varying concentrations of 2LM20-4, 2LM20-4 P331S or rituximab (data not shown).

Fig. 2 2LM20-4 has lower K_d and recruits fewer CD20 molecules than rituximab into lipid rafts. K_ds were determined using ^{125}Iodine-labelled 2LM20-4 or rituximab and primary B cells. Each K_d determination was repeated three times with the same donor. GraphPad Prism software was used for curve fitting. The total, 2LM20-4-specific and non-specific (**A**), or rituximab-specific and non-specific (**B**) binding is shown. (**C**) Scatchard plots for 2LM20-4 (curved) and rituximab (linear). (**D**) Ramos B cells were incubated with iodinated anti-CD20 molecules for 0–60 min. Cells pellets were lysed with 0.5% Triton X-100. Soluble and insoluble lysate fractions were counted on a gamma counter followed by the determination of the distribution of radio labelled proteins in the soluble *vs* insoluble fractions.

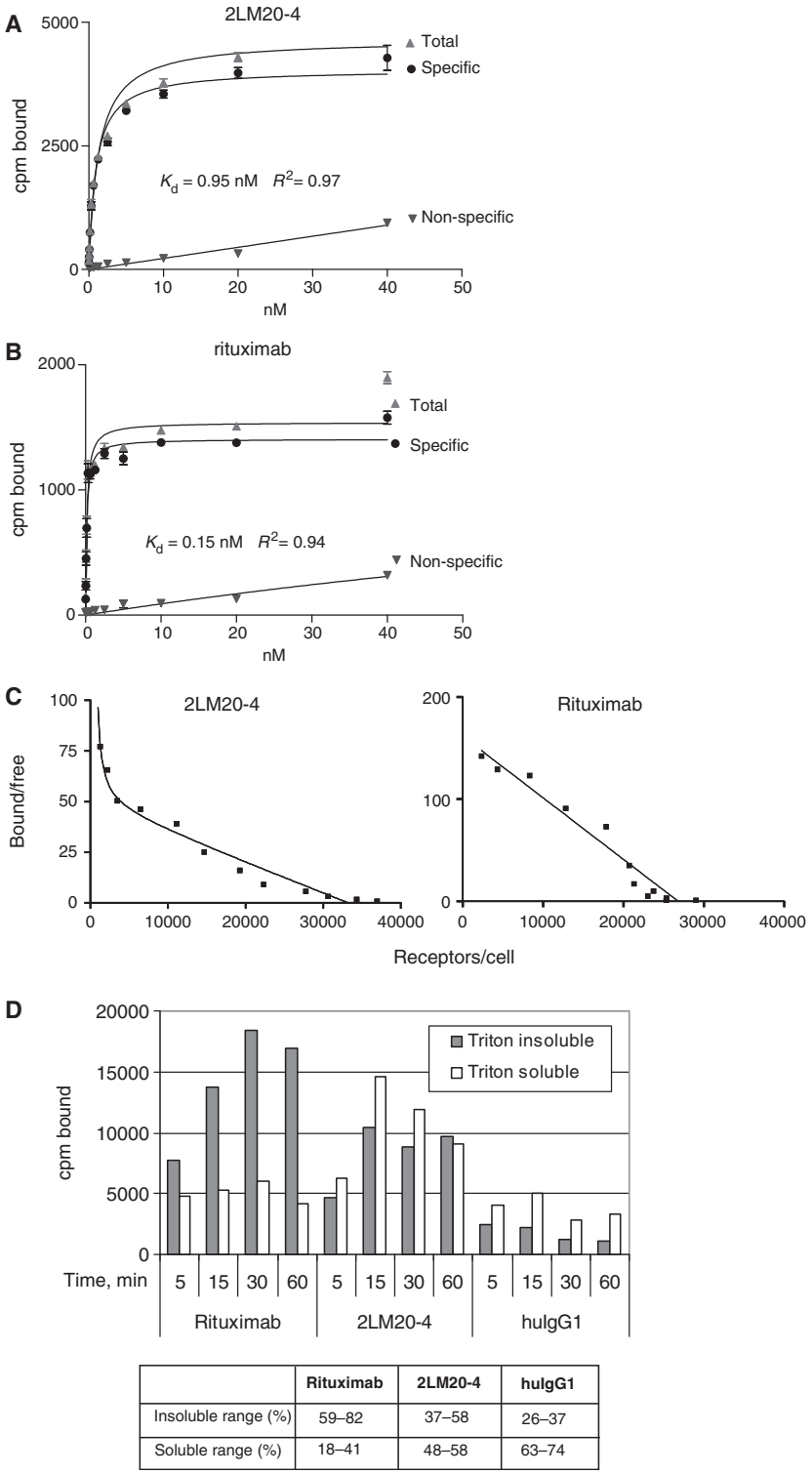

	Rituximab	2LM20-4	hulgG1
Insoluble range (%)	59–82	37–58	26–37
Soluble range (%)	18–41	48–58	63–74

FIG. 3 2LM20-4 shows partial displacement of rituximab in direct binding assays. (**A**) Excess of unlabelled 2LM20-4 only partially displaced ^{125}I-rituximab binding to CD20 on primary B cells. (**B**) B cells were treated for 1 and 24 h with biotinylated anti-CD20 molecules. The competitor was added first, and the biotinylated anti-CD20 added last. The cells were stained with Alexa Fluor 568-SA and aliquots were used for staining with 7AAD and CD19–APC and FACS analysis. (**C**) The rest of the cells were spun onto microscope slides, nuclei stained with TO-PRO 3 and cells visualized by confocal microscopy. The 1-h time point is shown.

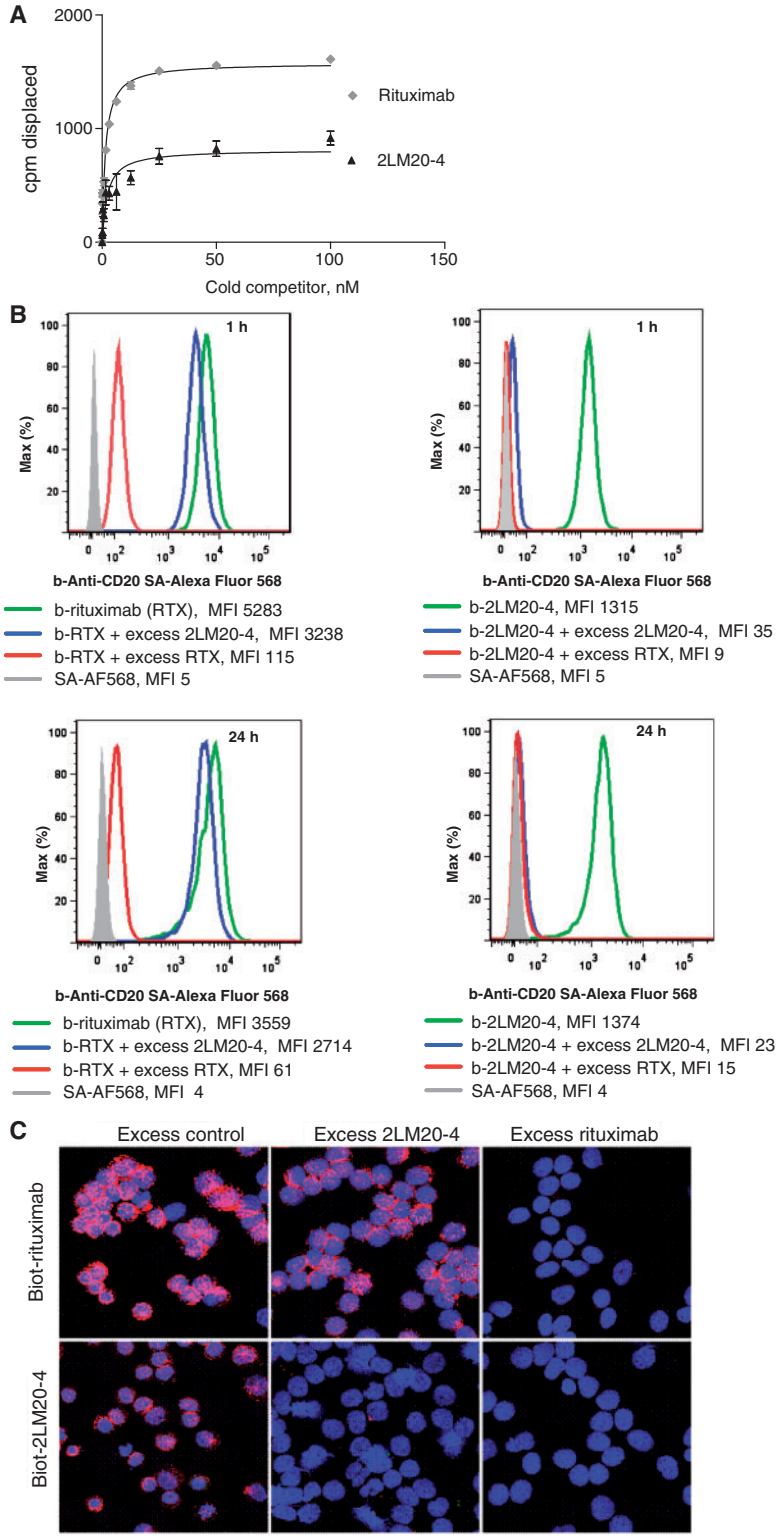

Fig. 4 2LM20-4 induces potent CDC and Fc-mediated cellular toxicity, but no PCD. (**A**) *In vitro* CDC of 2LM20-4, 2LM20-4 P331S, rituximab or control IgG1 on primary human B cells. (**B**) *In vitro* Fc-mediated cellular toxicity by 2LM20-4, 2LM20-4 P331S, rituximab or control IgG1 against primary human B cells in the presence of autologous NK cells (effectors). (**C**) PCD induction by 2LM20-4, 2LM20-4 P331S, rituximab or control IgG1 was assessed on primary human B cells after 22 h using flow cytometry. Similar results were obtained using different healthy donors; for each effector function results from one donor are shown.

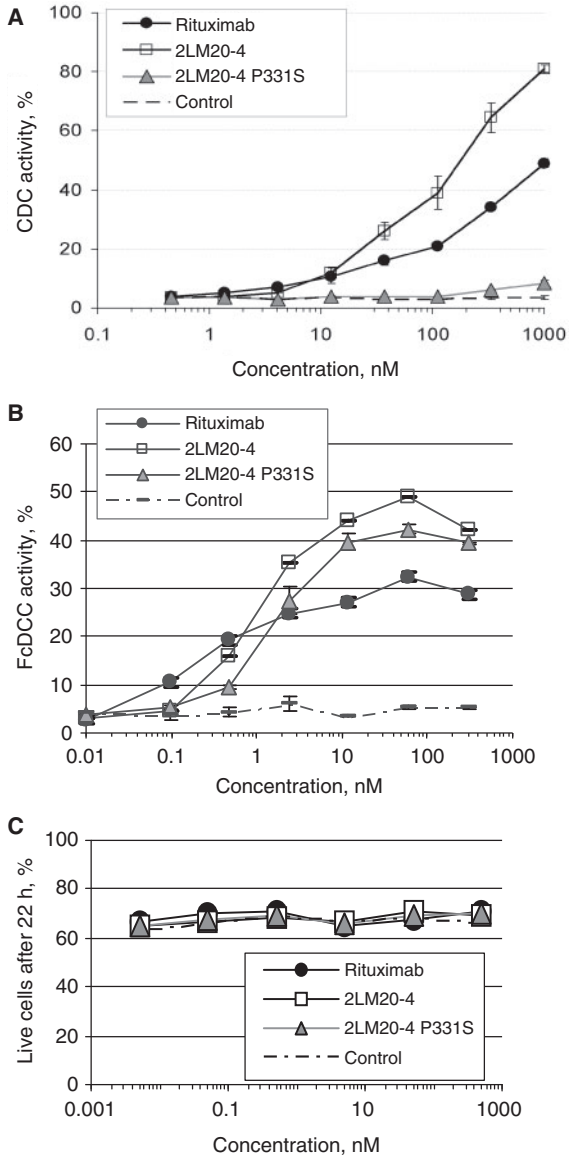

2LM20-4 has more potent and sustained peripheral CD19$^+$ B-cell depletion activity compared with rituximab

CD19$^+$ B-cell depletion and recovery in the peripheral blood of the cynomolgus monkeys that received 10 mg/kg of 2LM20-4, 2LM20-4 P331S or rituximab are shown in Fig. 5A. All three proteins had very potent and comparable activity during the first 3 weeks after dosing; however, significant B-cell recovery was observed earlier in the rituximab-treated group. All the groups had significant CD19$^+$ B-cell repletion by 6 months. The effect of a single i.v. 10 mg/kg dose of anti-CD20 molecules on the percentage of CD19$^+$ B cells in the bone marrow is shown in Fig. 5B. All the three proteins significantly decreased the percentage of CD19$^+$ B cells by Day 8. The percentage of CD19$^+$ B cells returned to baseline levels in the rituximab-treated monkeys by Day 22. In contrast, the percentage remained significantly decreased in the 2LM20-4 and 2LM20-4 P331S groups on Day 22. By the end of the study (D179), the number of CD19$^+$ B cells had returned to baseline levels in all of the groups. These results show that 2LM20-4 has very potent peripheral blood B-cell depletion activity, which is more sustained compared with 2LM20-4 P331S and rituximab, and that both SMIP proteins have more sustained depletion in the bone marrow compared with rituximab.

2LM20-4 demonstrates more potent and sustained lymph node CD19$^+$ B-cell depletion activity compared with 2LM20-4 P331S and rituximab

The effect of a single i.v. 10 mg/kg dose of 2LM20-4, 2LM20-4 P331S or rituximab on the percentage of CD19$^+$ B cells in the lymph nodes is shown in Fig. 6. There was a significant decrease in the number of CD19$^+$ B cells in the lymph nodes of all groups by Day 8. This depletion was more profound in the rituximab and 2LM20-4-treated groups with >75% depletion of the CD19$^+$ cells compared with 50% in the 2LM20-4 P331S group. By Day 29, the number of CD19$^+$ B cells had significantly increased in the rituximab group, but not in the 2LM20-4 and 2LM20-4 P331S groups. Notably, the 2LM20-4 group had even fewer CD19$^+$ B cells than on Day 8. By the end of the study, there was a full recovery in the percentage of CD19$^+$ cells in all groups. No changes were observed in the histopathology examination in each group by the end of the study (data not shown). Also, no differences were noted in CD3-, CD20- or CD68-positive cells in inguinal lymph nodes in any of the animals in Groups 3, 6 and 9 and in the vehicle group (data not shown). These results demonstrate that 2LM20-4 has significantly more potent activity in the lymph nodes compared with 2LM20-4 P331S and rituximab, indicating that, in addition to other mechanisms, CDC effector function has a major role in the elimination of lymph node B cells in cynomolgus monkeys.

Discussion

Work on the mechanisms of B-cell killing by anti-CD20 mAbs has categorized anti-CD20 mAbs as type I and the rare type II [14, 31]. Although this classification clearly encompasses a broad spectrum of the *in vitro* properties that have been attributed to anti-CD20 mAbs in previous reports, here we present evidence that 2LM20-4 cannot be classified either as a type I or a type II anti-CD20

Fig. 5 B-cell depletion activity of anti-CD20 molecules in the peripheral blood and bone marrow of cynomolgus monkeys. (**A**) Absolute numbers of $CD19^+$ B cells monitored in the peripheral blood with flow cytometry. *Significantly different from 2LM20-4 P331S and 2LM20-4; **significantly different from 2LM20-4 only; ***2LM20-4 significantly different from 2LM20-4 P331S and from rituximab; #all three groups are different from each other. (**B**) Kinetics of bone marrow $CD19^+$ B-cell depletion and recovery. *Significant from baseline acclimation values at $P < 0.05$ by a linear mixed model analysis. All data are presented as the mean (S.D.) percentage of $CD19^+$ lymphocytes relative to acclimation Day 7 (A7).

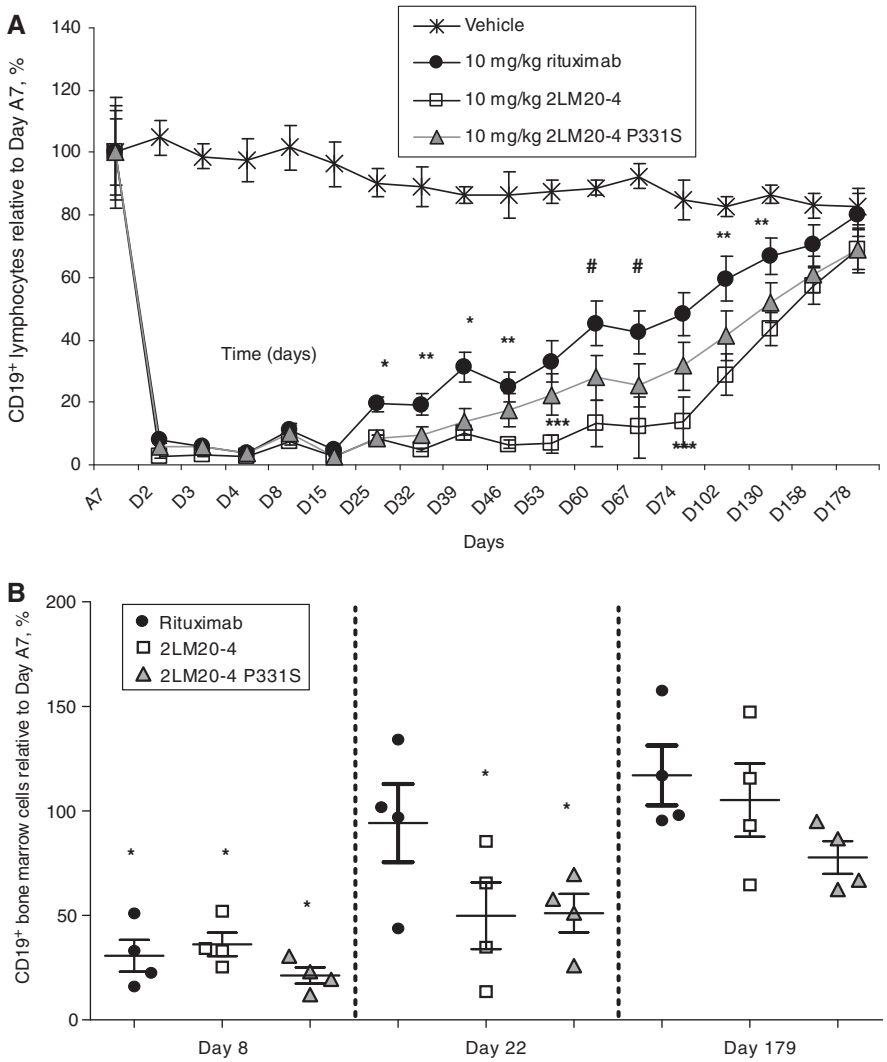

molecule. 2LM20-4 binds to significantly fewer CD20 molecules on primary B cells compared with rituximab, as shown by flow cytometry, direct binding and confocal assays (Fig. 1C and D). These data would suggest that 2LM20-4 primarily binds to CD20 molecules in soluble regions of the plasma membrane, whereas rituximab is able to interact with, or drive CD20 into insoluble regions. Also, the competition experiments suggest that 2LM20-4 is able to compete rituximab bound to CD20 preferentially in soluble regions of the plasma membrane. It is possible that the higher binding affinity (Fig. 2A and B) of rituximab results in increased binding of CD20 in insoluble areas as compared with 2LM20-4. Another possible interpretation for the lower saturation binding of 2LM20-4 in Fig. 1C and D is that, due to the intrinsic nature of the SMIP scaffold, it can simultaneously bind to two molecules of CD20, and, therefore, it only necessitates half the amount of protein required to occupy the available CD20 molecules compared with rituximab. However, the competition binding assays do not support this hypothesis, as a 100-fold molar excess of 2LM20-4 only partially displaces rituximab (Fig. 3A–C). Overall, these finding suggest that 2LM20-4 and rituximab may recognize differentially localized CD20 molecules, which results in the different staining levels and patterns observed in cells. This is also supported by our Triton X-100 findings, which show that 2LM20-4 recruits significantly fewer CD20 molecules into lipid rafts compared with rituximab (Fig. 2C). Recently, it

Fig. 6 B-cell depletion activity of anti-CD20 molecules in lymph nodes of cynomolgus monkeys**.** Kinetics of lymph node $CD19^+$ B-cell depletion and recovery were analysed with flow cytometry at the indicated time points. Data are presented as the mean (S.D.) percentage of $CD19^+$ lymphocytes relative to acclimation Day 7 (A7). *Significant from baseline acclimation values at $P < 0.05$ by a linear mixed model analysis; **significantly different between indicated groups at <0.05 by a linear mixed model analysis.

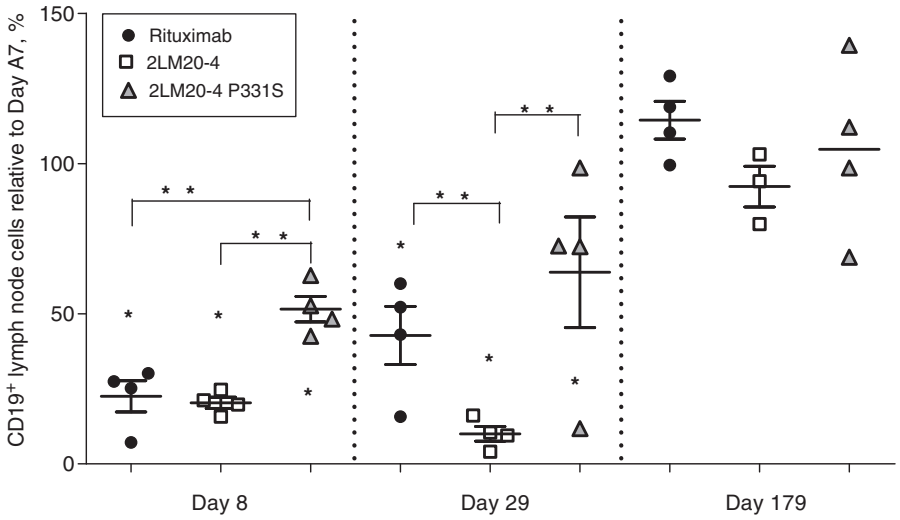

has been shown that homotypic adhesion followed by lysosome-mediated cell death are the mechanisms underlying B-cell death induced by type II anti-CD20 mAbs [31]. 2LM20-4 has none of these type II characteristics: it has no ability to induce homotypic adhesion of either primary B cells or B-cell lymphoma lines, as assessed by light microscopy (data not shown), and does not initiate PCD in either primary B cells (Fig. 4C) or B-cell lymphoma lines (data not shown).

It is noteworthy that 2LM20-4 has increased CDC as compared with rituximab despite its higher off-rate (data not shown) and its reduced ability to recruit CD20 into Triton-insoluble microdomains. Previous reports have shown that the activation of the large hexameric glycoprotein C1q requires fixation of its globular heads at an angle that favours autoactivation of the tetrameric C1rC1s components [32]. Thus, the CDC activity of 2LM20-4, as of most anti-CD20 mAbs, may be attributable to the small size of the extracellular domain of CD20 and can be explained by critical dependence on the distance between the plasma membrane and the constant regions of the sensitizing antibody [33, 34]. In this regard, the SMIP structure of 2LM20-4 offers a potential explanation for its more potent CDC compared with rituximab, as it may deliver C1q closer to the cell membrane. Teeling *et al.* [35] had initially proposed that the off-rate of the mAb controls the amount of C1q that binds on the cell surface. 2LM20-4 has fast off-rate (data not shown), and this may facilitate its re-binding to B cells and activation of complement, leading ultimately to higher CDC activity. In support of this is the longer half-life ($t_{½}$) of 2LM20-4 compared with rituximab [7.8 ± 1.5 and 5.4 ± 2.0 days in the 10 mg/kg dose groups, respectively; data not shown]. Teeling *et al*. [35] also determined that the locality at which complement is activated, and the epitope on CD20 also could play a role [16]. 2LM20-4 originates from the 2H7 mouse antibody, which was epitope mapped and was shown to recognize a similar epitope to rituximab [16]. Despite this overlapping in binding epitopes, our results of cell-surface binding and competition experiments suggest that 2LM20-4 recognizes only a proportion of CD20 molecules on the B cells. Overall, we conclude that the distinct binding properties of 2LM20-4 that can be attributed, at least partially, to its modular SMIP configuration, may favour capturing of C1q via multiple globular heads, thus holding it long enough in a conformation that is required for autoactivation and induction of potent CDC activity. The question remains whether it is the binding domain with its higher off-rate or the SMIP structure that more efficiently mediates complement-induced killing of cells.

In the *in vivo* cynomolgus monkey B-cell depletion model, both 2LM20-4 and 2LM20-4 P331S have favourable pharmacokinetic profiles (data not shown) and equally potent B-cell depletion activity in the peripheral blood and bone marrow, which is more sustained than that observed with rituximab. Most importantly, 2LM20-4 has significantly higher activity in the lymph nodes compared with 2LM20-4 P331S, and significantly prolonged activity compared with rituximab, indicating that CDC activity may be required for more effective B-cell depletion in some tissues of cynomolgus monkeys. These findings are in agreement with the concept that the mechanism of B-cell depletion may vary with different compartments and indicates that B cells within lymphoid tissues that have reduced circulatory capacity might exhibit a greater dependence on complement- rather than Fc receptor-mediated mechanisms for

depletion. These results point to two major conclusions: first, the *in vitro* binding properties of an anti-CD20 molecule are not predictive of its *in vivo* B-cell depletion potency: 2LM20-4 binds to only a fraction of CD20 molecules as compared with rituximab; however, 2LM20-4 appears to have more potent and sustained B-cell depletion activity in the cynomolgus monkey study. Secondly, high CDC activity is required for more potent and sustained B-cell depletion in lymphoid tissues, as 2LM20-4 has significantly more potent and sustained activity compared not only with 2LM20-4 P331S, but also with rituximab in cynomolgus monkeys.

In conclusion, we have shown that SMIP 2LM20-4, which has a distinct *in vitro* binding profile, has profound and sustained B-cell depletion activity in cynomolgus monkeys. These results provide fresh insight into how anti-CD20 molecules may potentiate their *in vitro* and *in vivo* B-cell depletion activity and indicate that 2LM20-4 represents a very promising B-cell-depleting drug candidate with unique properties that support clinical evaluation in patients with B-cell-dependent autoimmune disorders.

Rheumatology key messages

- *In vitro* binding to CD20 is not predictive of *in vivo* B-cell depletion potency.
- CDC activity is required for potent B-cell depletion in lymph nodes of cynomolgus monkeys.
- SMIP 2LM20-4 represents a promising B-cell-depleting drug candidate for treatment of autoimmune diseases.

Acknowledgements

The authors would like to thank Dr Lixin Han for the detailed statistical analysis of the data, Christopher Shea and Nicole Duriga for bioanalytical support and Dr Quint Medley for critically reviewing the article.

Funding: The study was funded by Pfizer, Inc.

Disclosure statement: C.N.-N., L.T., N.P.S., M.K., B.S., S.O., R.Z., D.H., Y.V., D.W., N.M.W., D.G., M.C. and K.D.-J. were employees of Pfizer Inc. during the time this work was performed and, therefore, were receiving salary and/or holding stock in Pfizer. W.A.B., K.M.M., P.B. and A.W. were employees of Trubion Pharmaceuticals during the time this work was performed and, therefore, were receiving salary and/or holding stock in Trubion.

References

1 Edwards JC, Cambridge G. B-cell targeting in rheumatoid arthritis and other autoimmune diseases. Nat Rev Immunol 2006;6:394–403.

2 Mandik-Nayak L, Ridge N, Fields M, Park AY, Erikson J. Role of B cells in systemic lupus erythematosus and rheumatoid arthritis. Curr Opin Immunol 2008;6:639–45.

3 Mease PJ. B cell-targeted therapy in autoimmune disease: rationale, mechanisms, and clinical application. J Rheumatol 2008;35:1245–55.

4 Yanaba K, Bouaziz JD, Matsushita T, Magro CM, St Clair EW, Tedder TF. B-lymphocyte contributions to human autoimmune disease. Immunol Rev 2008;223:284–99.

5 Dorner T, Radbruch A, Burmester GR. B-cell-directed therapies for autoimmune disease. Nat Rev Rheumatol 2009;5:433–41.

6 Cohen SB, Emery P, Greenwald MW *et al*. Rituximab for rheumatoid arthritis refractory to anti-tumor necrosis factor therapy: results of a multicenter, randomized, double-blind, placebo-controlled, phase III trial evaluating primary efficacy and safety at twenty-four weeks. Arthritis Rheum 2006;54:2793–806.

7 Anolik JH, Barnard J, Owen T *et al*. Delayed memory B cell recovery in peripheral blood and lymphoid tissue in systemic lupus erythematosus after B cell depletion therapy. Arthritis Rheum 2007;56:3044–56.

8 Jonsdottir T, Gunnarsson I, Risselada A, Henriksson EW, Klareskog L, van Vollenhoven RF. Treatment of refractory sle with rituximab plus cyclophosphamide: clinical effects, serological changes, and predictors of response. Ann Rheum Dis 2008;67:330–4.

9 Ng KP, Cambridge G, Leandro MJ, Edwards JC, Ehrenstein M, Isenberg DA. B cell depletion therapy in systemic lupus erythematosus: long-term follow-up and predictors of response. Ann Rheum Dis 2007;66:1259–62.

10 Favas C, Isenberg DA. B-cell-depletion therapy in SLE–what are the current prospects for its acceptance? Nat Rev Rheumatol 2009;5:711–6.

11 Stuve O, Leussink VI, Frohlich R *et al*. Long-term B-lymphocyte depletion with rituximab in patients with relapsing-remitting multiple sclerosis. Arch Neurol 2009;66:259–61.

12 Hauser SL, Waubant E, Arnold DL *et al*. B-cell depletion with rituximab in relapsing-remitting multiple sclerosis. N Engl J Med 2008;358:676–88.

13 Pescovitz MD, Greenbaum CJ, Krause-Steinrauf H *et al*. Rituximab, B-lymphocyte depletion, and preservation of beta-cell function. N Engl J Med 2009;361:2143–52.

14 Glennie MJ, French RR, Cragg MS, Taylor RP. Mechanisms of killing by anti-CD20 monoclonal antibodies. Molecular Immunology 2007;44:3823–37.

15 Beers SA, Chan CH, James S *et al*. Type II (tositumomab) anti-CD20 monoclonal antibody out performs type I (rituximab-like) reagents in B-cell depletion regardless of complement activation. Blood 2008;112:4170–7.

16 Teeling JL, Mackus WJ, Wiegman LJ *et al*. The biological activity of human CD20 monoclonal antibodies is linked to unique epitopes on cd20. J Immunol 2006;177:362–71.

17 Ghetie MA, Bright H, Vitetta ES. Homodimers but not monomers of rituxan (chimeric anti-CD20) induce apoptosis in human B-lymphoma cells and synergize with a chemotherapeutic agent and an immunotoxin. Blood 2001;97:1392–8.

18 Clynes RA, Towers TL, Presta LG, Ravetch JV. Inhibitory fc receptors modulate in vivo cytoxicity against tumor targets. [see comment]. Nature Medicine 2000;6:443–6.

19 Di Gaetano N, Cittera E, Nota R *et al*. Complement activation determines the therapeutic activity of rituximab in vivo. J Immunol 2003;171:1581–7.

20 Cragg MS, Glennie MJ. Antibody specificity controls in vivo effector mechanisms of anti-CD20 reagents. Blood 2004;103:2738–43.

21 Golay J, Cittera E, Di Gaetano N *et al*. The role of complement in the therapeutic activity of rituximab in a murine B lymphoma model homing in lymph nodes. [see comment]. Haematologica 2006;91:176–83.

22 Gong Q, Ou Q, Ye S *et al*. Importance of cellular microenvironment and circulatory dynamics in B cell immunotherapy. J Immunol 2005;174:817–26.

23 Eisenberg R, Looney RJ. The therapeutic potential of anti-cd20 ''what do B-cells do?'' Clin Immunol 2005;117: 207–13.

24 Boumans MJ, Tak PP. Rituximab treatment in rheumatoid arthritis: how does it work? Arthritis Res Ther 2009;11:134.

25 Blank M, Shoenfeld Y. B cell targeted therapy in autoimmunity. J Autoimmun 2007;28:62–8.

26 Liu AY, Robinson RR, Hellstrom KE, Murray ED Jr, Chang CP, Hellstrom I. Chimeric mouse-human IgG1 antibody that can mediate lysis of cancer cells. Proc Natl Acad Sci 1987;84:3439–43.

27 Polyak MJ, Deans JP. Alanine-170 and proline-172 are critical determinants for extracellular CD20 epitopes; heterogeneity in the fine specificity of CD20 monoclonal antibodies is defined by additional requirements imposed by both amino acid sequence and quaternary structure. Blood 2002;99:3256–62.

28 Deans JP, Robbins SM, Polyak MJ, Savage JA. Rapid redistribution of cd20 to a low density detergent-insoluble membrane compartment. J Biol Chem 1998;273:344–8.

29 Xu Y, Oomen R, Klein MH. Residue at position 331 in the IgG1 and IgG4 CH2 domains contributes to their differential ability to bind and activate complement. J Biol Chem 1994;269:3469–74.

30 Janas E, Priest R, Wilde JI, White JH, Malhotra R. Rituxan (anti-CD20 antibody)-induced translocation of CD20 into lipid rafts is crucial for calcium influx and apoptosis. Clin Exp Immunol 2005;139:439–46.

31 Ivanov A, Beers SA, Walshe CA *et al*. Monoclonal antibodies directed to CD20 and HLA-DR can elicit homotypic adhesion followed by lysosome-mediated cell death in human lymphoma and leukemia cells. J Clin Invest 2009;119:2143–59.

32 Schumaker VN, Zavodszky P, Poon PH. Activation of the first component of complement. Annu Rev Immunol 1987; 5:21–42.

33 Xia MQ, Hale G, Waldmann H. Efficient complement-mediated lysis of cells containing the campath-1 (CDw52) antigen. Mol Immunol 1993;30: 1089–96.

34 Bindon CI, Hale G, Bruggemann M, Waldmann H. Human monoclonal IgG isotypes differ in complement activating function at the level of C4 as well as C1q. J Exp Med 1988; 168:127–42.

35 Teeling JL, French RR, Cragg MS *et al*. Characterization of new human CD20 monoclonal antibodies with potent cytolytic activity against non-hodgkin lymphomas. Blood 2004;104:1793–800.